



# Iron Isotope Constraints on the Structure of the Early Solar System

Yves Marrocchi<sup>1</sup> , Maxime Piralla<sup>1,2</sup> , and François L. H. Tissot<sup>3</sup> <sup>1</sup> Centre de recherches pétrographiques et géochimiques (CRPG), CNRS, UMR 7358, F-54000, Nancy, France; [yvesm@crpg.cnrs-nancy.fr](mailto:yvesm@crpg.cnrs-nancy.fr)<sup>2</sup> Max Planck Institute for Solar System Research, Justus-von-Liebig-Weg 3, D-37077 Göttingen, Germany<sup>3</sup> The Isotoparium, Division of Geological and Planetary Sciences, California Institute of Technology, Pasadena, CA 91125, USA

Received 2023 July 31; revised 2023 August 10; accepted 2023 August 13; published 2023 September 1

## Abstract

The recent advent of nontraditional isotopic systems has revealed that meteorites display a fundamental isotopic dichotomy between noncarbonaceous (NC) and carbonaceous (C) groups, which represent material from the inner and outer solar system, respectively. On the basis of iron isotope anomalies, this view has recently been challenged in favor of a circumsolar disk structured into three distinct reservoirs (the so-called isotopic trichotomy). In this scenario, the CI chondrites—a rare type of carbonaceous chondrites with chemical composition similar to that of the Sun’s photosphere—would sample a distinct source region than other carbonaceous chondrites, located beyond Saturn’s orbit. Here, we report a model based on the available data for both mass-dependent fractionation of Te stable isotopes and mass-independent Fe nucleosynthetic anomalies. On the basis of the Te–Fe isotopic correlation defined by all carbonaceous chondrites including CIs, we show that the NC–CC dichotomy extends to Fe isotopes. Our finding thus supports (i) the existence of only two reservoirs in the early solar system and (ii) the ubiquitous presence of CI-like dust throughout the carbonaceous reservoir. Our approach also reveals that the carrier phase of <sup>54</sup>Fe anomalies corresponds to Fe–Ni metal beads mostly located within chondrules. Finally, we propose that the CC chondrule component records a constant mix of refractory inclusions and NC-like dust.

*Unified Astronomy Thesaurus concepts:* Asteroids (72); Chondrites (228); Isotopic abundances (867); Meteorite composition (1037); Planet formation (1241); Planetary science (1255); Small Solar System bodies (1469); Solar system (1528)

## 1. Introduction

Protoplanetary disks (PPDs) are inevitable byproducts of stellar formation processes due to the conservation of angular momentum during molecular cloud collapse and fragmentation. They represent the birth cradles of planets, whose formation and properties are inherently entangled with the structure and physicochemical conditions of their respective parent PPDs. Understanding the configuration and evolution of PPDs is thus of fundamental importance for understanding planetesimal formation (Dullemond et al. 2018). While current astronomical observations can only rarely observe planets embedded in their PPDs directly (Benisty et al. 2021), recent high-resolution (sub) millimeter-wavelength telescopic images of <1 Myr old disks have revealed multiple dust ring structures (Andrews et al. 2018). These gaps and rings appear to be ubiquitous features of PPDs, yet the mechanisms at their origin remain unclear. Numerous scenarios have been proposed including clearing by embedded planets (Carrasco-González et al. 2016), dust growth in condensation zones or snow lines (Zhang et al. 2015), self-induced dust pileups (Gonzalez et al. 2017) or anisotropic infall (Kuznetsova et al. 2022). In any case, these observations suggest that PPDs are highly structured and composed of different reservoirs with potentially limited interactions between them.

Meteorites as recorders of the earliest stages of accretion and disk evolution in our own infant solar system make for a formidable complement to the astronomical observations. In particular, the recent finding of a fundamental isotopic dichotomy among all meteorites, irrespective of whether they

derive from differentiated or undifferentiated planetesimals, holds key constraints with regard to protosolar disk structure and its evolution (Warren 2011; Kruijer et al. 2017; Burkhardt et al. 2019). This dichotomy into so-called noncarbonaceous (NC) and carbonaceous (C) solar system materials stems from the bimodal distribution of nucleosynthetic isotope anomalies (e.g., in Ti, Cr, Mo, and Ni) among the meteorites. Thanks to chronological constraints on the formation timing of iron meteorites, it was shown that the NC–C meteoritic parent bodies formed in two spatially separated but temporally coexisting disk reservoirs (Warren 2011; Kruijer et al. 2017). By analogy to the astronomical observations of disk rings, the NC and C reservoirs are thus thought to represent distinct parts of the solar PPD (Kruijer et al. 2020), with the NC and C reservoirs respectively representing the inner and outer regions of the solar system. The barrier separating the inner (NC) from the outer (C) reservoir has been attributed to the early formation of Jupiter’s core (Kruijer et al. 2017), a long-lived pressure maximum (Brasser & Mojzsis 2020), or evolving ice and silicate lines in the disk (Lichtenberg et al. 2021; Morbidelli et al. 2022). As the nature of the NC/C barrier is debated, so is its permeability, and current inferences range from a hard barrier with almost no influx of outer solar system material to the inner disk, to a soft barrier with large amounts of outer solar system dust passing through the inner disk toward the Sun (Kruijer et al. 2020; Schiller et al. 2020; Hopp et al. 2022a).

The recent analyses of samples brought back from the Cb-type asteroid 162173 Ryugu by the JAXA’s Hayabusa2 space mission revealed mineralogical, chemical and isotopic similarities with CI chondrites (Yokoyama et al. 2022). Although Ryugu and CI chondrites correspond to an endmember of the C meteorite reservoir in <sup>50</sup>Ti–<sup>54</sup>Cr–O isotope space, they, however, plot in the continuation of the trend defined by other



Original content from this work may be used under the terms of the [Creative Commons Attribution 4.0 licence](https://creativecommons.org/licenses/by/4.0/). Any further distribution of this work must maintain attribution to the author(s) and the title of the work, journal citation and DOI.

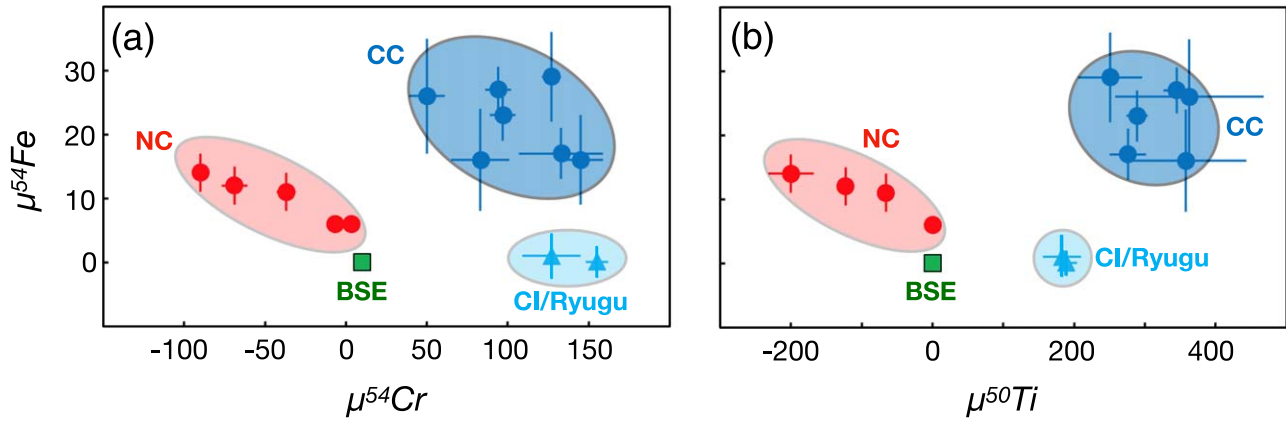


**Figure 1.** Diagrams of  $\mu^{54}\text{Cr}$  vs.  $\mu^{54}\text{Fe}$  (a) and  $\mu^{50}\text{Ti}$  vs.  $\mu^{54}\text{Fe}$  (b) for the bulk silicate Earth (BSE, green, Ryugu samples (pale blue), NC (red), and C (blue) chondrites. Error bars correspond to group average and their respective standard errors (2SE) of the mean (95%). Ryugu/CI samples appear somehow disconnected from other CCs and were interpreted as suggesting the presence of an isotopic dichotomy in the early solar system (Hopp et al. 2022a). Data from Burkhardt et al. (2021), Hopp et al. (2022a, 2022b), and Schiller et al. (2020).

carbonaceous chondrites (hereafter CC; Kruijer et al. 2020). Conversely, the Fe isotopic anomalies of Ryugu/CIs are significantly distinct from those of other CCs (Figure 1; Schiller et al. 2020; Hopp et al. 2022a, 2022b). Based on these results, it has been proposed that Ryugu/CIs are unique meteorites representing an isotopically distinct third reservoir located beyond the orbit of Saturn (Hopp et al. 2022a), thus suggesting the existence of an isotopic trichotomy between NC, C, and CI meteorites (Hopp et al. 2022a). However, recent modeling suggest that this apparent NC-C-CI trichotomy might arise from the current lack of Fe isotope data for C achondrites (Yap & Tissot 2023).

In this contribution, we use the available data for both mass-dependent fractionation of stable isotopes (Te; Hellmann et al. 2020) and mass-independent nucleosynthetic anomalies ( $^{54}\text{Fe}$  and  $^{54}\text{Cr}$ , Schiller et al. 2020; Hopp et al. 2022a, 2022b) to address the number of early solar system reservoirs (dichotomy versus trichotomy). We show that Ryugu/CIs represent an endmember in a  $\delta^{128}\text{Te}$ - $\mu^{54}\text{Fe}$  diagram, thus supporting the structuration of the solar system in only two reservoirs instead of three as proposed by the elusive isotopic trichotomy. We also discuss the implications of our findings on the (i) nature of the primitive matrix accreted by carbonaceous chondrites, (ii) spatial distribution of both nucleosynthetic anomalies and CI-like dust in the disk, and (iii) conditions of chondrule formation.

## 2. Correlated Elemental and Isotopic Variations among CCs

Compared to the large and well-documented  $^{50}\text{Ti}$  and  $^{54}\text{Cr}$  nucleosynthetic anomalies,  $^{54}\text{Fe}$  variations in meteorites show more subtle variations and were reported only recently (Schiller et al. 2020; Hopp et al. 2022a, 2022b). Consideration of the  $^{50}\text{Ti}$ - $^{54}\text{Fe}$ - $^{54}\text{Cr}$  systematics has led to the proposition of the existence of an isotopic trichotomy in the solar system, as Ryugu and CI samples plot far away from other CC in both  $^{50}\text{Ti}$ - $^{54}\text{Fe}$  and  $^{54}\text{Cr}$ - $^{54}\text{Fe}$  diagrams (Figure 1). One cannot exclude that this trichotomy results from the currently limited Fe isotopic data, especially for CC achondrites that could bridge the gap between Ryugu/CIs and other CCs (Yap & Tissot 2023). To test this idea, we follow a simple approach based on the available data for both the iron abundance and  $^{54}\text{Fe}$  isotopic compositions in CCs.

We first consider the Fe concentrations reported for all CCs as well as for the Ryugu samples (Braukmüller et al. 2018; Yokoyama et al. 2022). Plotting along with the modal abundance of matrix (expressed as mass fraction), Fe concentrations in CC chondrites define a negative trend, with Ryugu/CIs being the least iron-rich samples (Figure 2(a)). This is in stark contrast to the systematic positive correlations observed between matrix mass fraction and abundances of volatile and moderately volatile elements in CCs (e.g., Rb, K, Zn, Te; Hellmann et al. 2020; Nie et al. 2021). Nevertheless, it allows calculating the iron concentration of the nonmatrix component, inferred from the intercept at matrix fraction of zero, to be  $24.38 \pm 1.51$  wt% (Figure 2(a)). To constrain the Fe isotopic composition of the nonmatrix component, we extrapolate the mixing relationship between the mu values and the reciprocals of the elemental concentrations to the Fe concentration estimated above (Figure 2(b)). This yields a  $\mu^{54}\text{Fe}$  for the nonmatrix component of  $32.9 \pm 13.3$  ppm (Figure 2(b)). Within error, this value is similar to those of the only two CC chondrules measured to date (i.e.,  $37.4 \pm 5.9$  ppm and  $42.4 \pm 8.5$  ppm for two CR chondrules; Schiller et al. 2020). This strongly suggests that the  $^{54}\text{Fe}$ -excess-bearing nonmatrix component likely correspond to chondrules. Interestingly, the magnitude of the  $^{54}\text{Fe}$  anomalies observed in CCs is also correlated with the inverse of nickel concentration (Figure 3). This supports the idea that the carrier of  $^{54}\text{Fe}$  anomalies correspond to the large Fe-Ni metal beads of few tens of microns, which represent minor but ubiquitous chondrule constituents in all CC groups (Jones 2012). We expect that these metal beads will also be the carrier phase of Ni anomalies (Burkhardt et al. 2021).

Determining the nature of the primitive matrix accreted by CCs is of primary importance as it may hold important information on the origin of dust in the solar PPD (Leroux et al. 2015). Whereas bulk CCs exhibit CI (=solar) chondritic Mg/Si ratios (Lodders 2003), chondrules and matrices have super- and sub-CI chondritic ratios, respectively (Palme et al. 2015). Although being intensively debated (e.g., Zanda et al. 2018), this is generally interpreted as resulting from a chondrule/matrix complementarity consequential to their formation from a unique chemical reservoir of solar composition (Palme et al. 2015). At the same time, the recent  $\delta^{128}\text{Te}$ - $\mu^{54}\text{Cr}$  correlated variations among CCs (Figure 4(a); Hellmann et al. 2020) reflect binary mixing of isotopically distinct endmembers,

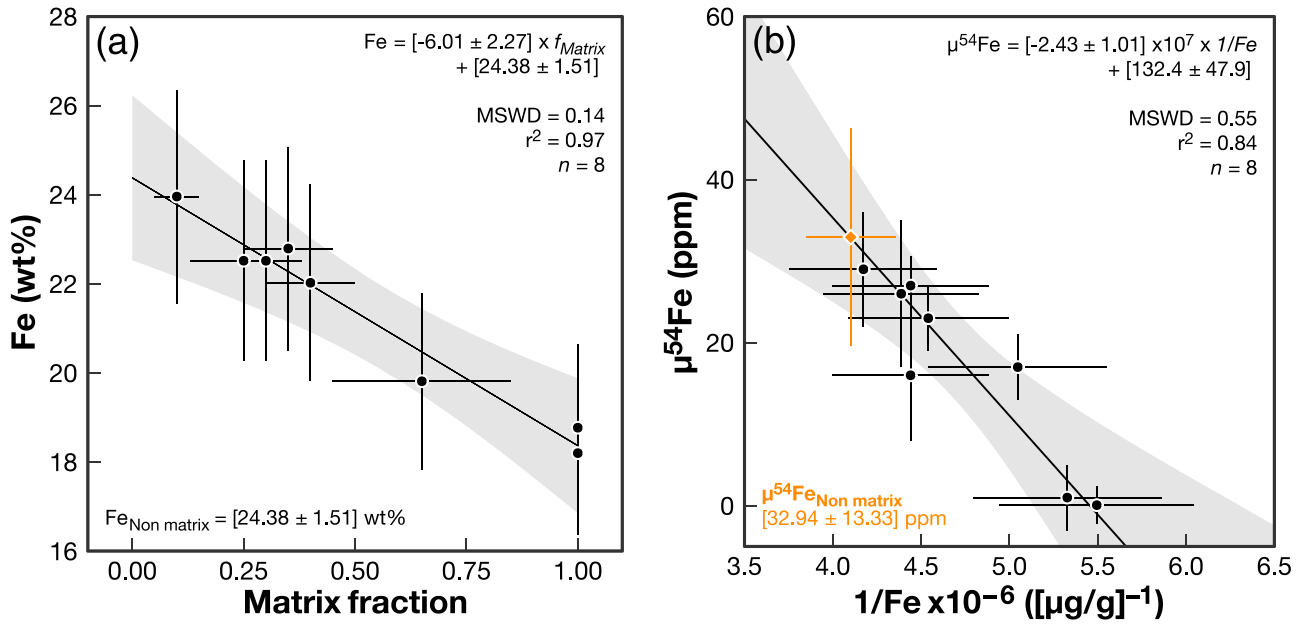


**Figure 2.** (a)—Average Fe concentration of carbonaceous chondrites as a function of the mass fraction of matrix. The regression corresponds to the best fits using weight errors and assuming a 10% error on the Fe concentration. The regression intercept allows estimating the Fe concentration of the nonmatrix component to be  $24.38 \pm 1.51$  wt%. Iron concentration from Braukmüller et al. (2018). Matrix mass fraction from Hellmann et al. (2020). (b)— $\mu^{54}Fe$  vs.  $1/Fe$  ( $\times 10^{-6}$ ) mixing line defined by carbonaceous chondrites.  $1/Fe$  was calculated using abundances in  $\mu g/g$ . The Fe isotopic composition of the nonmatrix component ( $32.9 \pm 13.3$ ) was determined using the inferred Fe concentration. Error on this component was estimated using a Monte Carlo approach. The regression corresponds to the best fit using weighted errors.

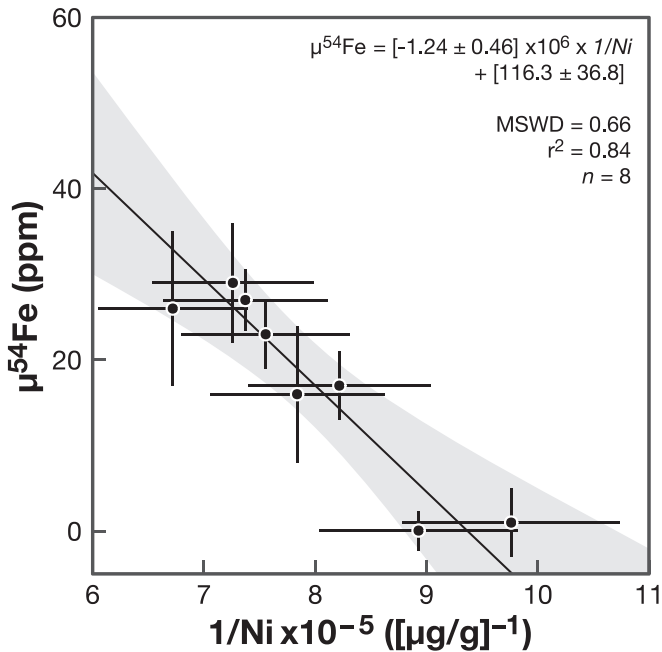


**Figure 3.** Average Ni concentration of carbonaceous chondrites as a function of the mass fraction of matrix. The regression corresponds to the best fits using weight errors and assuming a 10% error on the Ni concentration. This suggests that the  $^{54}Fe$  anomalies in CCs are carried by Fe–Ni metal beads. Iron concentration from Braukmüller et al. (2018). Matrix mass fraction from Hellmann et al. (2020).

corresponding to CI-like matrix and a nonmatrix component being likely associated to chondrules (Hellmann et al. 2020; Marrocchi et al. 2022). Similar isotopic relationships have been also reported for moderately volatile elements such as K, Zn, and Rb (Luck et al. 2005; Pringle et al. 2017; Nie et al. 2021). This thus rather supports that all CCs accreted CI-like matrix, whose

respective abundance controls the bulk concentrations of volatile and moderately volatile elements in CCs. Our examination of the data shows that the  $^{54}Fe$  variations observed among CCs also correlate with the Te isotopic compositions (Figure 4(b); Hellmann et al. 2020). This implies that the Fe isotopic anomalies in CCs are also controlled by a binary mixing, with CI-like dust being a ubiquitous component that likely corresponds to the primordial matrix accreted by all CCs. One can note that both CO and CR chondrites plot slightly off the mixing hyperbola (Figure 4(b)). The latter offset likely results from the occurrence of two chondrule generations in CR chondrites as recently proposed on the basis of O–Cr–Te isotopic systematics (Marrocchi et al. 2022). Considering CO chondrites, their average  $^{54}Fe$  value ( $\mu^{54}Fe = 16 \pm 8$  ppm,  $n = 4$ ) is impacted by the lower iron anomaly reported for Kainsaz (i.e.,  $\mu^{54}Fe = 9 \pm 4$  ppm; Schiller et al. 2020) compared to other COs chondrites (average  $\mu^{54}Fe = 18.5 \pm 2.2$  ppm,  $n = 3$ , 2SE, Hopp et al. 2022a). Despite these uncertainties, our finding shows that, similarly to other isotopic systems, the iron isotopic anomalies among CCs are controlled by a binary mixing between CI-like matrix and a chondrule component.

### 3. Implications for the Structure and the Dynamic of the Protoplanetary Disk

A major feature of the isotopic dichotomy lies in the fact that it holds for elements having drastically different geochemical (i.e., lithophile/siderophile) and thermal (i.e., refractory/moderately volatile) behaviors (Burkhardt et al. 2021; Steller et al. 2022). The Fe isotope anomalies, however, show an apparent gap between Ryugu/CIs and other CCs (Figure 1; Schiller et al. 2020; Hopp et al. 2022a, 2022b). This was interpreted as representing a potential isotopic trichotomy with Ryugu/CI samples being unique specimens sampling a third, previously unrecognized reservoir, positioned beyond the orbit

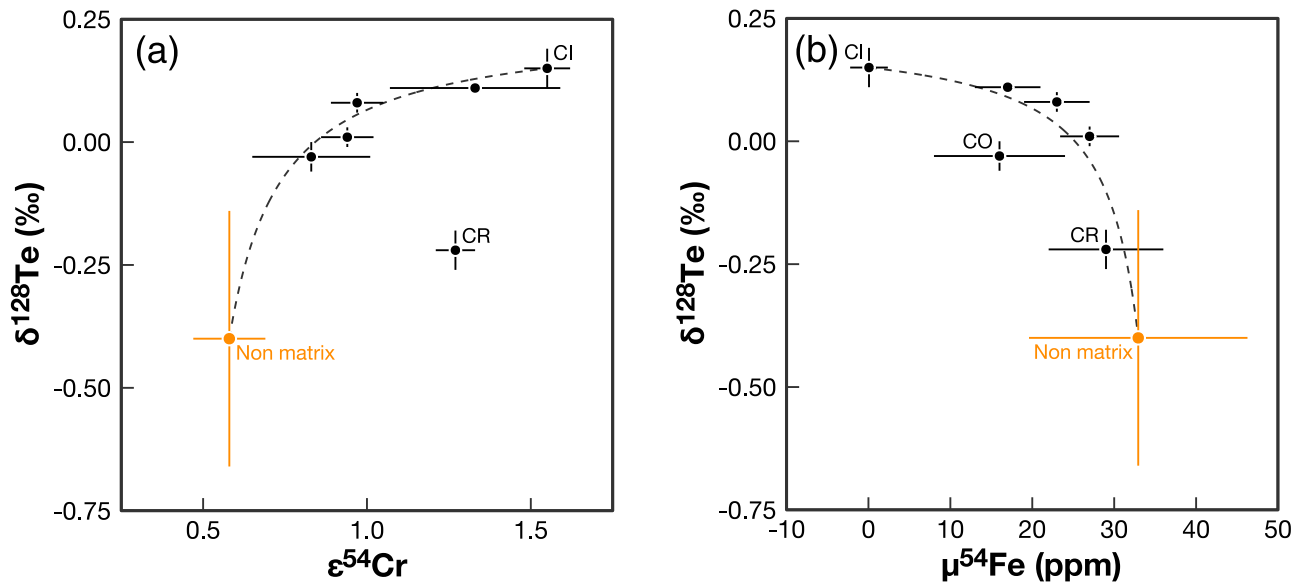


**Figure 4.** (a)— $\delta^{128/126}\text{Te}$  vs.  $\epsilon^{54}\text{Cr}$  trend defined by all CCs. The dashed curve corresponds to the mixing hyperbola calculated by taking into account the respective Te and Cr concentrations and isotopic compositions of CI and the nonmatrix components (data from Hellmann et al. 2020; Burkhardt et al. 2021). (b)— $\delta^{128/126}\text{Te}$  vs.  $\epsilon^{54}\text{Fe}$  trend established from all CCs. The mixing hyperbola is calculated from the Te and Fe concentrations and isotopic compositions.

of Saturn (Hopp et al. 2022a). In this model, the growth and migration of gas and ice giant planets result in the destabilization of the CC and Ryugu/CI parent bodies that were (i) scattered inward and outward in the disk and (ii) partially implanted in the main asteroidal belt (Hopp et al. 2022a). Our observations do not, however, support this interpretation. Similar to the Te–Cr isotopic correlation observed among CCs (Figure 4(a); Hellmann et al. 2020), we show that the Te isotopic compositions of carbonaceous chondrites are also correlated with nucleosynthetic  $^{54}\text{Fe}$  anomalies (Figure 4(b)). As Ryugu/CIs represent an isotopic endmember in the  $\delta^{128}\text{Te}-\epsilon^{54}\text{Fe}$  diagram (Figure 4(b)), this implies that all CCs have accreted CI-like matrix, likely in the form of fine-grained material dispersed throughout the PPD that will ultimately accrete as CC matrices. Our finding thus supports models proposing that Ryugu/CIs and other CCs belong to the same outer solar system reservoir (Bryson & Brennecke 2021; Yap & Tissot 2023). It also shows that CI-like material represents a major component of the C reservoir, as also inferred from (i) the bulk chemical compositions of CCs (Braukmüller et al. 2018) and (ii) models based on the CC nucleosynthetic anomaly systematics (Bryson & Brennecke 2021; Hellmann et al. 2023; Yap & Tissot 2023). Altogether, this attests that CIs are much more abundant than their small occurrences in our collections tell us ( $n = 9$ ), as all CCs are partially composed of fine-grained CI-like matrix. This implies a paradigm shift where CI-like dust should be now considered as the most abundant material of the outer solar system in our collections, which could represent the background composition of the molecular cloud parental to the solar system as recently postulated (Yap & Tissot 2023). The only singularity of the Ryugu/CI samples finally stands in the limited number of high-temperature components such calcium–aluminum-rich inclusions (CAIs)/ameboid olivine aggregates (AOAs) and chondrules they accreted compared to other CCs (Piralla et al. 2020; Morin et al. 2022; Nakamura et al. 2022). In that sense, CI chondrites *sensu stricto* can be considered as a specific type of chondrites, somehow disconnected from other CCs, but not representing a hypothetical third isolated reservoir. Their

scarcity on Earth lies in their (i) accretion in the very outer reaches of the solar system (Desch et al. 2018) and (ii) their brittle nature and their consequent inability to pass through the terrestrial atmospheric filter.

One outcome of our model is to show that the carrier phase of  $^{54}\text{Fe}$  anomalies likely corresponds to Fe–Ni metal beads, as attested by the relationship between the iron anomalies and the Ni contents (Figure 3). Within CCs, Fe–Ni metal beads mostly occurs in chondrules (Jones 2012) although large Fe–Ni metal beads also befall around chondrules and as isolated in their matrices (Campbell et al. 2005). Large grains outside of chondrules have, however, similar chemical compositions to that of chondrule metal beads and were thus likely expelled during their formation processes (Campbell et al. 2005; Jacquet et al. 2013). Hence, it is reasonable to assume that metal-bearing chondrule represent the main carrier phase of Fe isotope anomalies as attested by the large  $^{54}\text{Fe}$  excesses reported in two CR chondrules (Schiller et al. 2020). The lack of  $^{54}\text{Fe}$  excess in Ryugu/CIs compared to other CCs thus suggest that chondrules only represent a marginal component of these samples.

The fact that CC chondrules represent an isotopic endmember in the respective  $\delta^{128}\text{Te}-\epsilon^{54}\text{Cr}$  and  $\delta^{128}\text{Te}-\epsilon^{54}\text{Fe}$  diagrams (Figure 4) has important implications on the (i) spatial distribution of nucleosynthetic anomalies in the disk and (ii) the location and conditions of chondrule formation. It first indicates that the Fe and Cr isotopic compositions of bulk CCs are controlled by the relative amount of chondrules and matrix in each group, the Cr and Fe concentrations in CAIs and AOAs being too low to disrupt the chondrule–matrix mixing hyperbolas (Figure 4). Second, this implies that all CC chondrules have near-constant isotopic composition across most chondrite groups, at the notable exception of CR chondrites that experienced more complex chondrule formation processes (Hellmann et al. 2020, 2023; Bryson & Brennecke 2021; Marrocchi et al. 2022). At first order, this feature could be interpreted as resulting from the formation of all CC chondrules in a similar region before being dispersed throughout the disk. This is, however, unlikely as CC chondrules show significant



petrological differences across CC groups (e.g., elemental compositions, textures, sizes; Jones 2012).

Alternatively, the unique isotopic value of CC chondrule component (Figure 4) provides important information on the distribution of nucleosynthetic anomalies in chondrule-forming regions. Based on oxygen isotopes and nucleosynthetic anomalies, it has been proposed that CC porphyritic chondrules partially derived from AOAs through the addition of NC-like dust (Jacquet & Marrocchi 2017; Marrocchi et al. 2018, 2019; Schneider et al. 2020; Villeneuve et al. 2020; Jacquet et al. 2021). Al-rich chondrules are also believed to have formed via the recycling of CAIs due to their high refractory element content (Ebert et al. 2018). Hence, this implies that the chondrule component represent a mixture between CAIs/AOAs and NC-like dust with a fixed ratio for all CCs. Altogether, this attests that the chondrule-forming regions were homogeneous in terms of nucleosynthetic anomalies (on average), irrespective of the abundance of CI-like matrix. The picture that emerges is that of a relatively homogeneous outer disk, with a constant CAIs+AOAs/NC ratio and ubiquitously populated by CI-like dust. Importantly, the major differences between the nucleosynthetic isotopic compositions of CAIs/AOAs and chondrules require a change in the isotopic composition of material infalling from the molecular cloud (Nanne et al. 2019). Our approach suggests that this major change affected the whole outer reservoir with a spatially constant contribution of NC-like material that significantly changed the compositional signature of the earliest disk recorded by both CAIs and AOAs.




#### 4. Concluding Remarks

Nucleosynthetic anomalies in meteorites are key tracers for quantifying transport and mixing processes in the early solar system and has revealed the existence of two distinct reservoirs in the early solar system. This isotopic dichotomy has been, however, recently called into question on the basis of the distinct Fe isotopic anomalies reported between Ryugu/CI samples and all other carbonaceous chondrites. This was interpreted as evidence of the existence of three reservoirs in the circumsolar disk, with Ryugu/CI material sampling a distant reservoir beyond Saturn's orbit. Based on previously published Te–Fe isotopic data, we show that the Te isotopic compositions of carbonaceous chondrites correlate with nucleosynthetic  $^{54}\text{Fe}$  anomalies. As Ryugu/CIs represent an isotopic endmember in the  $\delta^{128}\text{Te}-\epsilon^{54}\text{Fe}$  diagram, our approach shows that the NC-CC dichotomy extends to Fe isotopes. This thus supports (i) the existence of only two reservoirs in the early solar system and (ii) the ubiquitous presence of CI-like dust throughout the carbonaceous reservoir. We also propose that the carrier phase of  $^{54}\text{Fe}$  anomalies corresponds to Fe–Ni metal beads mostly located within chondrules. Finally, our approach suggests that the CC chondrule component records a constant mix of refractory inclusions and NC-like dust.

#### Acknowledgments

David V. Bekaert, Gabriel Pinto, and Johan Villeneuve are thanked for helpful discussions. James Bryson is thanked for helpful review and Brian Jackson for careful editing. This is CRPG contribution #2849.

#### ORCID iDs

Yves Marrocchi  <https://orcid.org/0000-0001-7075-3698>  
 Maxime Piralla  <https://orcid.org/0000-0001-9332-6250>  
 François L. H. Tissot  <https://orcid.org/0000-0001-6622-2907>

#### References

- Andrews, S. M., Huang, J., Pérez, L. M., et al. 2018, *ApJL*, 869, L41  
 Benisty, M., Bae, J., Facchini, S., et al. 2021, *ApJL*, 916, L2  
 Brasser, R., & Mojzsis, S. J. 2020, *NatAs*, 4, 492  
 Braukmüller, N., Wombacher, F., Hezel, D. C., Escoube, R., & Münker, C. 2018, *GeCoA*, 239, 17  
 Bryson, J. F. J., & Brennecke, G. A. 2021, *ApJ*, 912, 163  
 Burkhardt, C., Dauphas, N., Hans, U., Bourdon, B., & Kleine, T. 2019, *GeCoA*, 261, 145  
 Burkhardt, C., Spitzer, F., Morbidelli, A., et al. 2021, *SciA*, 7, eabj7601  
 Campbell, A. J., Zanda, B., Perron, C., Meibom, A., & Petaev, M. I. 2005, in ASP Conference Series Vol. 341, Chondrites and the Protoplanetary Disk, ed. A. N. Krot, E. R. D. Scott, & B. Reipurth (San Francisco, CA: ASP), 407  
 Carrasco-González, C., Henning, T., Chandler, C. J., et al. 2016, *ApJL*, 821, L16  
 Desch, S. J., Kalyaan, A., & Alexander, C. M. O. 2018, *ApJ*, 238, 11  
 Dullemond, C. P., Birnstiel, T., Huang, J., et al. 2018, *ApJL*, 869, L46  
 Ebert, S., Render, J., Brennecke, G. A., et al. 2018, *E&PSL*, 498, 257  
 Gonzalez, J.-F., Laibe, G., & Maddison, S. T. 2017, *MNRAS*, 467, 1984  
 Hellmann, J. L., Hopp, T., Burkhardt, C., & Kleine, T. 2020, *E&PSL*, 549, 116508  
 Hellmann, J. L., Schneider, J. M., Wölfer, E., et al. 2023, *ApJL*, 946, L34  
 Hopp, T., Dauphas, N., Abe, Y., et al. 2022a, *SciA*, 8, eadd8141  
 Hopp, T., Dauphas, N., Spitzer, F., Burkhardt, C., & Kleine, T. 2022b, *E&PSL*, 577, 117245  
 Jacquet, E., & Marrocchi, Y. 2017, *M&PS*, 52, 2672  
 Jacquet, E., Paulhiac-Pison, M., Alard, O., Kearsley, A. T., & Gounelle, M. 2013, *M&PS*, 48, 1981  
 Jacquet, E., Piralla, E., Kersaho, P., & Marrocchi, Y. 2021, *M&PS*, 56, 13  
 Jones, R. H. 2012, *M&PS*, 47, 1176  
 Kruijer, T. S., Burkhardt, C., Budde, G., & Kleine, T. 2017, *PNAS*, 114, 6712  
 Kruijer, T. S., Kleine, T., & Borg, L. E. 2020, *NatAs*, 4, 32  
 Kuznetsova, A., Bae, J., Hartmann, L., & Low, M.-M. M. 2022, *ApJ*, 928, 92  
 Leroux, H., Cuvillier, P., Zanda, B., & Hewins, R. H. 2015, *GeCoA*, 170, 247  
 Lichtenberg, T., Drażkowska, J., Schönbachler, M., Golabek, G. J., & Hands, T. O. 2021, *Sci*, 371, 365  
 Lodders, K. 2003, *ApJ*, 591, 1220  
 Luck, J.-M., Othman, D. B., & Albarède, F. 2005, *GeCoA*, 69, 5351  
 Marrocchi, Y., Euverte, R., Villeneuve, J., et al. 2019, *GeCoA*, 247, 121  
 Marrocchi, Y., Piralla, M., Regnault, M., et al. 2022, *E&PSL*, 593, 117683  
 Marrocchi, Y., Villeneuve, J., Batanova, V., et al. 2018, *E&PSL*, 496, 132  
 Morbidelli, A., Baillié, K., Batygin, K., et al. 2022, *NatAs*, 6, 72  
 Morin, G. L. F., Marrocchi, Y., Villeneuve, J., & Jacquet, E. 2022, *GeCoA*, 332, 203  
 Nakamura, E., Kobayashi, K., Tanaka, R., et al. 2022, *PJAB*, 98, 227  
 Nanne, J. A. M., Nimmo, F., Cuzzi, J. N., & Kleine, T. 2019, *E&PSL*, 511, 44  
 Nie, N. X., Chen, X.-Y., Hopp, T., et al. 2021, *SciA*, 7, eabl3929  
 Palme, H., Hezel, D. C., & Ebel, D. S. 2015, *E&PSL*, 411, 11  
 Piralla, M., Marrocchi, Y., Verdier-Paoletti, M. J., et al. 2020, *GeCoA*, 269, 451  
 Pringle, E. A., Moynier, F., Beck, P., Paniello, R., & Hezel, D. C. 2017, *E&PSL*, 468, 62  
 Schiller, M., Bizzarro, M., & Siebert, J. 2020, *SciA*, 6, eaay7604  
 Schneider, J. M., Burkhardt, C., Marrocchi, Y., Brennecke, G. A., & Kleine, T. 2020, *E&PSL*, 551, 116585  
 Steller, T., Burkhardt, C., Yang, C., & Kleine, T. 2022, *Icar*, 386, 115171  
 Villeneuve, J., Marrocchi, Y., & Jacquet, E. 2020, *E&PSL*, 542, 116318  
 Warren, P. H. 2011, *E&PSL*, 311, 93  
 Yap, T. E., & Tissot, F. L. H. 2023, *Icar*, 405, 115680  
 Yokoyama, T., Nagashima, K., Nakai, I., et al. 2022, *Sci*, 379, 7850  
 Zanda, B., Lewin, E., & Humayun, M. 2018, in Chondrules, ed. S. S. Russell, H. C. Connolly, Jr., & A. N. Krot (Cambridge: Cambridge Univ. Press), 122  
 Zhang, K., Blake, G. A., & Bergin, E. A. 2015, *ApJL*, 806, L7